



**QUEEN'S
UNIVERSITY
BELFAST**

Integrated gut metabolome and microbiome fingerprinting reveals that dysbiosis precedes allergic inflammation in IgE-mediated pediatric cow's milk allergy

De Paepe, E., Plekhova, V., Vangeenderhuysen, P., Baeck, N., Bullens, D., Claeys, T., De Graeve, M., Kamoen, K., Notebaert, A., Van de Wiele, T., Van Den Broeck, W., Vanlede, K., Van Winckel, M., Vereecke, L., Elliott, C., Cox, E., & Vanhaecke, L. (2024). Integrated gut metabolome and microbiome fingerprinting reveals that dysbiosis precedes allergic inflammation in IgE-mediated pediatric cow's milk allergy. *Allergy*. Advance online publication. <https://doi.org/10.1111/all.16005>

Published in:
Allergy

Document Version:
Publisher's PDF, also known as Version of record

Queen's University Belfast - Research Portal:
[Link to publication record in Queen's University Belfast Research Portal](#)

Publisher rights

Copyright 2024 the authors.

This is an open access article published under a Creative Commons Attribution-NonCommercial-NoDerivs License (<https://creativecommons.org/licenses/by-nc-nd/4.0/>), which permits distribution and reproduction for non-commercial purposes, provided the author and source are cited.

General rights

Copyright for the publications made accessible via the Queen's University Belfast Research Portal is retained by the author(s) and / or other copyright owners and it is a condition of accessing these publications that users recognise and abide by the legal requirements associated with these rights.

Take down policy

The Research Portal is Queen's institutional repository that provides access to Queen's research output. Every effort has been made to ensure that content in the Research Portal does not infringe any person's rights, or applicable UK laws. If you discover content in the Research Portal that you believe breaches copyright or violates any law, please contact openaccess@qub.ac.uk.

Open Access

This research has been made openly available by Queen's academics and its Open Research team. We would love to hear how access to this research benefits you. – Share your feedback with us: <http://go.qub.ac.uk/oa-feedback>

Integrated gut metabolome and microbiome fingerprinting reveals that dysbiosis precedes allergic inflammation in IgE-mediated pediatric cow's milk allergy

Ellen De Paepe¹ | Vera Plekhova¹ | Pablo Vangeenderhuysen¹ | Nele Baeck² | Dominique Bullens^{3,4} | Tania Claeys⁵ | Marilyn De Graeve¹ | Kristien Kamoen⁶ | Anneleen Notebaert⁷ | Tom Van de Wiele⁸ | Wim Van Den Broeck⁹ | Koen Vanlede¹⁰ | Myriam Van Winckel¹¹ | Lars Vereecke^{11,12,13} | Chris Elliott¹⁴ | Eric Cox¹⁵ | Lynn Vanhaecke^{1,14} 

¹Faculty of Veterinary Medicine, Department of Translational Physiology, Infectiology and Public Health, Laboratory of Integrative Metabolomics (LIMET), Ghent University, Merelbeke, Belgium

²Department of Pediatrics, Pediatric Gastroenterology, AZ Jan Palfijn Ghent, Ghent, Belgium

³Department of Microbiology, Immunology and Transplantation, Allergy and Immunology Research Group, KU Leuven, Leuven, Belgium

⁴Clinical Division of Pediatrics, UZ Leuven, Leuven, Belgium

⁵Department of Pediatrics, Pediatric Gastroenterology and Nutrition & General Pediatric Medicine, AZ Sint-Jan Bruges, Bruges, Belgium

⁶Department of Pediatrics, Maria Middelaers Ghent, Ghent, Belgium

⁷Department of Pediatrics, Sint-Vincentius Hospital Deinze, Deinze, Belgium

⁸Faculty of Bioscience Engineering, Center for Microbial Ecology and Technology (CMET), Ghent University, Ghent, 9000, Belgium

⁹Faculty of Veterinary Medicine, Department of Morphology, Imaging, Orthopedics, Rehabilitation and Nutrition, Ghent University, Merelbeke, Belgium

¹⁰Department of General Pediatrics, VITAZ, Sint-Niklaas, Belgium

¹¹Faculty of Medicine and Health Sciences, Department of Internal Medicine and Pediatrics, Ghent University, Ghent, Belgium

¹²VIB-UGent Center for Inflammation Research, Ghent, Belgium

¹³Ghent Gut Inflammation Group (GGIG), Ghent, Belgium

¹⁴School of Biological Sciences, Institute for Global Food Security, Queen's University Belfast, Belfast, United Kingdom

¹⁵Faculty of Veterinary Medicine, Department of Translational Physiology, Infectiology and Public Health, Laboratory of Immunology, Ghent University, Merelbeke, Belgium

Correspondence

Lynn Vanhaecke, Faculty of Veterinary Medicine, Department of Translational Physiology, Infectiology and Public Health, Laboratory of Integrative Metabolomics, Ghent University, Salisburylaan 133, 9820 Merelbeke, Ghent, Belgium.
Email: lynn.vanhaecke@ugent.be

Funding information

Fonds Wetenschappelijk Onderzoek; Bijzonder Onderzoeksfonds UGent

Abstract

Background: IgE-mediated cow's milk allergy (IgE-CMA) is one of the first allergies to arise in early childhood and may result from exposure to various milk allergens, of which β -lactoglobulin (BLG) and casein are the most important. Understanding the underlying mechanisms behind IgE-CMA is imperative for the discovery of novel biomarkers and the design of innovative treatment and prevention strategies.

Methods: We report a longitudinal in vivo murine model, in which two mice strains (BALB/c and C57Bl/6) were sensitized to BLG using either cholera toxin or an oil

Abbreviations: CMA, cow's milk allergy; rRNA, ribosomal RNA.

This is an open access article under the terms of the [Creative Commons Attribution-NonCommercial-NoDerivs](https://creativecommons.org/licenses/by-nc-nd/4.0/) License, which permits use and distribution in any medium, provided the original work is properly cited, the use is non-commercial and no modifications or adaptations are made.

© 2024 The Authors. *Allergy* published by European Academy of Allergy and Clinical Immunology and John Wiley & Sons Ltd.

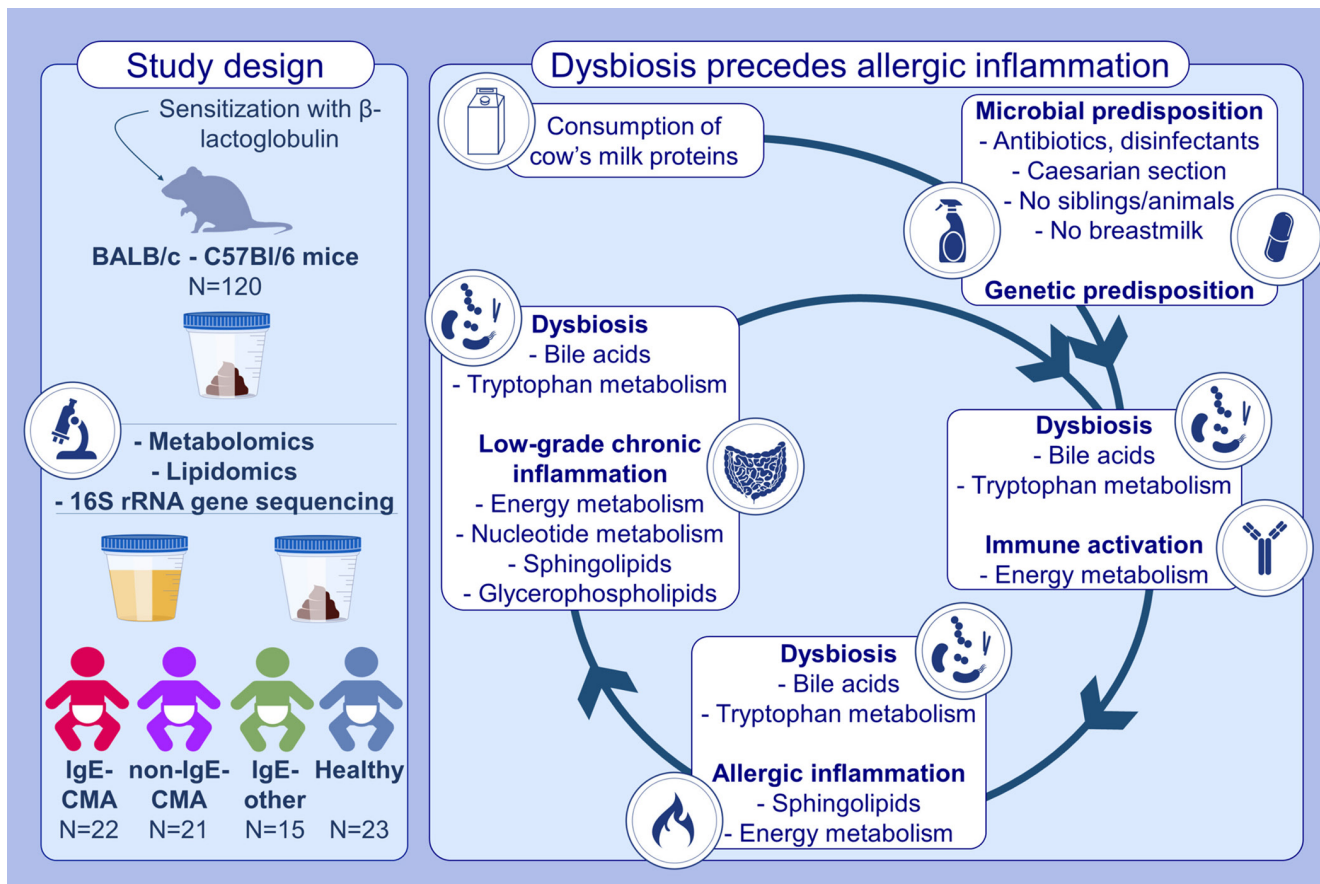
emulsion (n = 6 per group). After sensitization, mice were challenged orally, their clinical signs monitored, antibody (IgE and IgG1) and cytokine levels (IL-4 and IFN- γ) measured, and fecal samples subjected to metabolomics. The results of the murine models were further extrapolated to fecal microbiome-metabolome data from our population of IgE-CMA (n = 22) and healthy (n = 23) children (Trial: NCT04249973), on which polar metabolomics, lipidomics and 16S rRNA metasequencing were performed. In vitro gastrointestinal digestions and multi-omics corroborated the microbial origin of proposed metabolic changes.

Results: During mice sensitization, we observed multiple microbially derived metabolic alterations, most importantly bile acid, energy and tryptophan metabolites, that preceded allergic inflammation. We confirmed microbial dysbiosis, and its associated effect on metabolic alterations in our patient cohort, through in vitro digestions and multi-omics, which was accompanied by metabolic signatures of low-grade inflammation.

Conclusion: Our results indicate that gut dysbiosis precedes allergic inflammation and nurtures a chronic low-grade inflammation in children on elimination diets, opening important new opportunities for future prevention and treatment strategies.

KEYWORDS

16S rRNA sequencing, cow's milk allergy, metabolomics, multi-omics



GRAPHICAL ABSTRACT

Early-stage microbial metabolites, reflective of gut dysbiosis steer the development of the immune system toward food allergies. Allergic inflammation appears at the end of the sensitization through a dysregulation in sphingolipid and energy metabolism. Allergic children on an elimination diet suffer from subacute chronic inflammation, as a consequence of concurrent dysbiosis.

Abbreviations: CMA, cow's milk allergy; rRNA, ribosomal RNA

1 | INTRODUCTION

IgE-mediated cow's milk allergy (IgE-CMA) is one of the most frequently occurring food allergies (FAs) in children, with an increasing prevalence over the past few decades.^{1,2} Early-life sensitization to cow's milk proteins (CMP) is considered one of the first steps towards the "allergic march", that is., the occurrence of other Th2-related atopic manifestations later in life.³ Current diagnostic procedures only predict the likelihood of reaction, while the gold standard, the double-blind placebo-controlled food challenge, is time- and resource-intensive and carries an inherent risk of anaphylaxis.⁴ The mainstay of FA management remains strict dietary avoidance, potentially causing nutritional imbalances and growth problems.^{3,4} Various environmental factors, such as antibiotic usage, cesarean delivery, and dietary habits have been suggested to play a role in allergy development. Importantly, these factors are all linked to the gut microbiome, and the presence of dysbiosis has been demonstrated in IgE-mediated FA.⁵⁻¹⁵

In recent years, metabolomics has become an indispensable tool in revealing the missing link between the genome and human diseases,¹⁶ because it captures both an individual's genetic basis and the environmental factors that contribute to disease.^{16,17} Multiple metabolomics studies on FAs have identified metabolites in different biofluids that discriminate between disease state and severity, as summarized in our recent systematic review.⁴ To date, only one metabolomics study has been published on IgE-CMA focusing on feces and describing significant differences in the fecal microbiome and metabolome through adulthood.¹⁸ Indeed, the fecal metabolome provides the best functional readout of microbial activity and can be used as an intermediate phenotype reflecting diet-host-microbiome interactions.¹⁹

Using a multi-omics approach, we dissected the allergic response, by cataloguing sensitization-induced molecular changes in mice through fecal polar metabolomics and clinical findings, while fecal and urinary polar metabolomics, lipidomics, and 16S metagenomics were executed on a carefully designed pediatric cohort of allergic children ($n=81$). We tested two sensitization protocols in two mouse strains and profiled the molecular changes over time to reveal which model best mimics the human allergic response cascade and its underlying molecular mechanisms. In vitro gastrointestinal digestions of CMP and multi-omics data integration from the patient cohort results further corroborated the microbial nature of specific molecular changes.

2 | METHODS

2.1 | In vivo murine experiments

Murine experiments were approved by the Ghent University Hospital ethical committee (ECD 20-09) and performed according to European Community rules of animal care. Three- and six-week-old female BALB/c and C57Bl/6 mice were obtained from Charles River (Charles River Laboratories, Saint-Germain Nuelles, France). Following 1 week of acclimatization, mice were divided into different treatment groups ($n=6$ per group).

The first sensitization protocol was based on Adel-Patient et al., in which 4-week-old mice received oral gavages containing β -lactoglobulin (BLG) and cholera toxin (CT) once a week for 6 weeks²⁰ (Note S1, Figure S1). The second protocol was adapted from Shindo et al. and included intragastrical administration of BLG in PBS or oil emulsion, followed by intraperitoneal injection of sodium salicylate (SA). The latter protocol was performed 5x a week for 3 weeks (Note S1, Figure S2).²¹ One mouse (BLG in oil + SA) was lost on day 21.

Antigen challenge was performed on the day the mice were 70 days old. All groups were fasted overnight and treated orally twice (30 min apart) with 30 mg BLG in 0.1 mL PBS. Fecal samples for metabolomics were collected weekly from each mouse during sensitization and directly after antigen challenge. Plasma was collected for determination of BLG-specific IgE- and IgG1-antibodies, spleen for IFN- γ - and IL-4-measurements,^{9,20} and jejunum and ileum for histological examination (Note S1).

2.2 | Pediatric cohort

The central ethical committee of Ghent University Hospital approved all study protocols (EC2017/1634), as did the ethical committees of the additional centers (Bruges General Hospital Sint-Jan, Ghent General Hospital Jan Palfijn, Ghent General Hospital Maria Middelaers, Sint-Niklaas General Hospital VITAZ, Leuven University Hospital, and Deinze Sint-Vincentius Hospital). Patient selection criteria encompassed children (1) diagnosed with IgE-CMA, while the control groups encompassed children (2) diagnosed with other IgE-mediated FAs (IgE-other), (3) suspected of a CMA and consequently on a CMP-free diet, notwithstanding negative IgE-measurements, and (4) nonallergic siblings from the aforementioned groups. The latter was applied to account for both environmental and genetic predispositions to FA development. Food allergies were diagnosed by the treating physician and were based on a combination of methods, including open oral food challenges (OFC), which are commonly recommended in specialist allergy clinical practice²² and/or positive IgE-test results (skin prick tests, specific IgE-measurements, or both). Additionally, a recent history of IgE-mediated symptoms (skin-related reactions, gastrointestinal and respiratory symptoms, anaphylaxis) within 2 h after ingestion of the respective foods, and improvement upon elimination diet were considered. Children were further categorized based on the number of physician-diagnosed FAs (single vs. multiple) and their history of anaphylaxis. The presence of multiple FAs or a history of anaphylaxis were deemed as more severe phenotypes. Nonallergic control subjects had no personal history of IgE-mediated conditions (Note S2).

2.3 | In vitro gastrointestinal digestions

Two different CMP powder formulations were used, that is, Nutrilon 1 and Nutrilon Pepti 1 (Nutricia, Amsterdam, The Netherlands). Feces were obtained from six children within the original cohort

(<2 years old; 50% girls), without a history of antibiotic treatment 6 months prior to donation. Among the six participants, two children suffered from IgE-CMA, and two were designated as healthy controls. Two other children were initially diagnosed with IgE-CMA and were categorized as such in our patient cohort. However, at the time of the *in vitro* digestions, these patients no longer exhibited symptoms, indicating IgE-CMA resolution. *In vitro* simulation of the gastrointestinal digestion consisted of enzymatic digestion (mouth, stomach, and duodenum) followed by colonic fermentation. Preparation of fecal inocula, digestion fluids, and their incubations, were carried out as described by Van Hecke et al.²³ and Rombouts et al.²⁴ (Note S3). Samples were taken immediately following the addition of SHIME (Simulator of the Human Intestinal Microbial Ecosystem) medium and fecal inoculum in Brain Heart Infusion (BHI) medium (duodenal samples, T0) and after colonic digestion (T48) (Figure S3).

2.4 | Metabolomics

Urine and fecal samples were prepared and analyzed in a randomized order as previously described by De Paepe et al.²⁵ and Van Meulebroek et al.²⁶ Digestion samples were prepared according to Vanden Bussche et al.²⁷ and Rombouts et al.²⁴ and analyzed based on the validated UHPLC-Q-Orbitrap HRMS methods of Vanden Bussche et al.²⁷ and Van Meulebroek et al.²⁶ (Note S4.1). Targeted data processing was carried out with Xcalibur 3.0 software (Thermo Fischer Scientific, San José, CA, USA), whereby compounds were identified based on their *m/z*-value (mass deviation ≤ 5 ppm), and retention time relative to that of the authentic reference standard (Note S4.2, Tables S1–S3). Untargeted data interpretation was achieved using Compound Discoverer™ 3.1 (Thermo Fischer Scientific, San José, CA, USA) and SIMCA 14.1 (Umetrics AB, Sweden) software (Note S4.3). Biomarkers were annotated using spectral matching of the fragmentation data with the reference databases (Global Natural Products Social Molecular Networking (GNPS) ecosystem,²⁸ Compound Discoverer 3.1, MS2Query,²⁹ and SIRIUS4³⁰) (Note S4.4; Figure S4). Correlation analyses were performed through R version 3.4.3 integrated into our *in-house* data processing pipeline (<https://github.com/UGent-LIMET>; Table S4). Functional analysis was achieved with MetaboAnalyst 5.0³¹ using the mummichog algorithm with a permutation *p*-value cutoff of 0.25 and the KEGG reference library (*mus musculus* or *homo sapiens*).

2.5 | 16S rRNA gene sequencing

Microbiome DNA extraction was executed using QIAmp DNA Stool Mini kit (QIAGEN GmbH, Hilden, Germany) according to the manufacturer's instructions for pathogen detection (Note S5). Samples

were sent out to the company LGC Genomics GmbH (Teddington, Middlesex, UK) for library preparation and sequencing on an Illumina Miseq platform. Statistical analysis was achieved using MicrobiomeAnalyst 2.0³² (Note S5).

2.6 | Integrated data analysis

Integrated data analysis employed clinical, fecal and urinary polar metabolome, fecal lipidome, and microbiome data originating from our pediatric cohort or clinical and fecal polar metabolome data from the murine experiment. Spearman's correlation analysis³³ (FDR adjusted *p*-value <0.05) was executed to unravel those metabolic/lipid features (log transformed and pareto scaled) that displayed the highest interaction with individual OTUs (filtered and CLR transformed; $\rho > 0.3$) and specific IgE levels in the pediatric cohort and several immunological parameters (IgE, IgG1) in the murine experiment ($\rho > 0.5$). Multi-Omics Factor Analysis (MOFA)³⁴ and Data Integration for Biomarker Discovery using Latent Components (DIABLO)³⁵ were applied to discover the principal sources of variation in the multi-omic dataset of the pediatric cohort.

3 | RESULTS

3.1 | BALB/c mice sensitized with BLG and CT show a strong allergic response

Two sensitization protocols were tested on two different mice strains, in order to determine which model optimally resembled IgE-CMA in children. The latter was evaluated based on clinical - signs of anaphylaxis - and immunological - immunoglobulin G1 (IgG1), IgE, interferon- γ (IFN- γ), and interleukin-4 (IL-4) - responses. Following oral challenge, only the BALB/c group receiving BLG and CT in PBS ($n = 6$) expressed typical symptoms of anaphylaxis (Figure 1A; Table S5). In addition, these mice displayed significantly higher levels of BLG-specific IgG1 and IgE (*p*-value <0.001) (Figure 1B,C; Tables S6,S7). No differences were observed in IFN- γ and IL-4 levels after concanavalin A stimulation (Figure 1D; Tables S8,S9). One mouse did not display IgG1 and IgE responses and was removed from further data analysis. Histopathology of the jejunum evidenced mast cell degranulation, through the generalized detachment of epithelial cells from the basement membrane at the tips of the villi in mice receiving BLG and CT in PBS (Figure 1E–1H).³⁶ As C57Bl/6 mice and BALB/c mice treated with BLG in PBS or oil emulsion did not display any signs of anaphylaxis (Tables S10–S12), nor immunological responses, that is, formation of antibodies IgG1 and IgE (Tables S6,S7; S13,S14) or cytokines IFN- γ and IL-4 (Tables S8,S9; S15,S16), these were not retained as possible models for IgE-CMA in children.

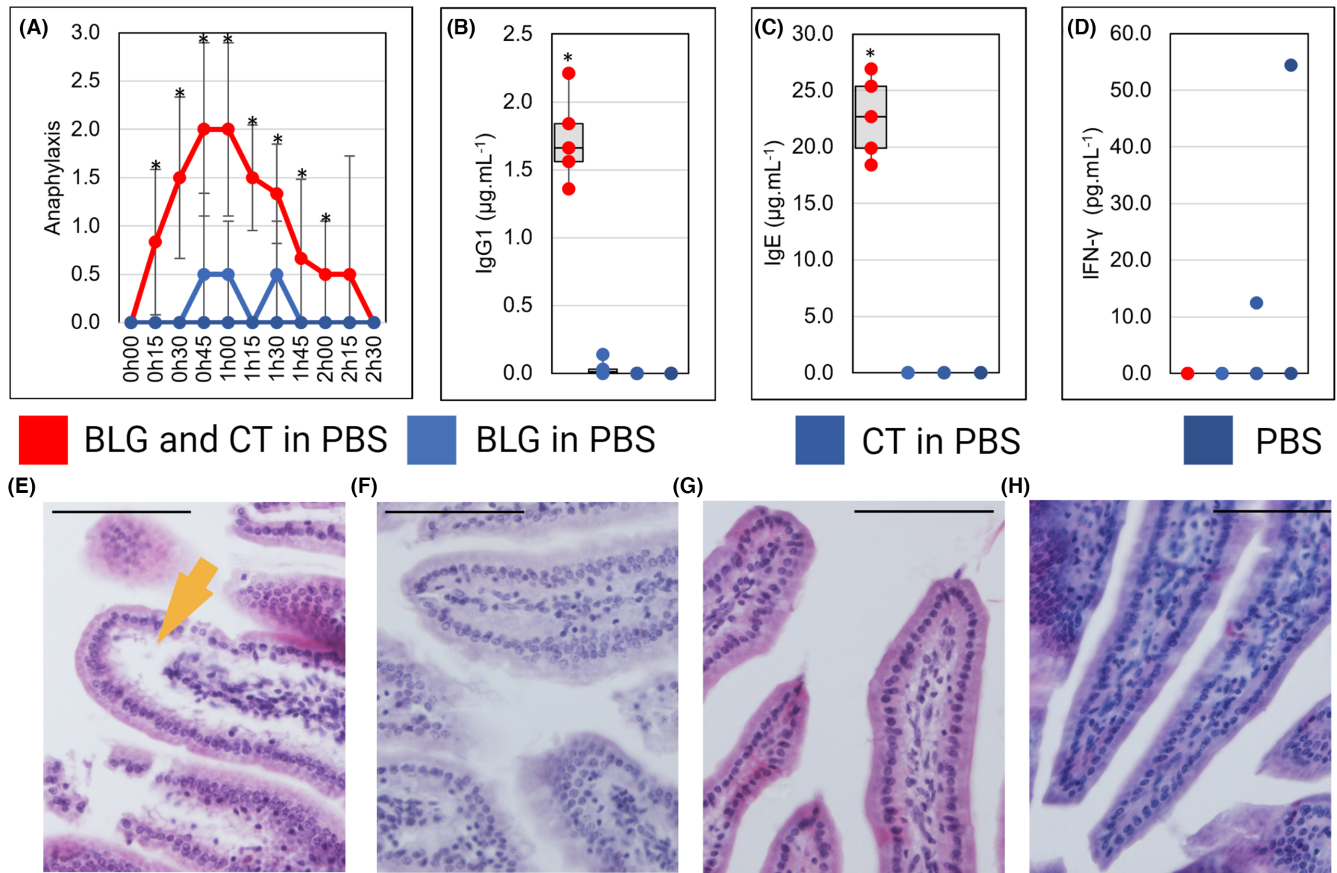


FIGURE 1 BALB/c mice sensitized with β -lactoglobulin (BLG) and cholera toxin (CT) in phosphate-buffered saline (PBS) show a strong allergic response following the antigen challenge. (A). Anaphylaxis score of the sensitized group compared to the control groups (0=no symptoms; 1=scratching and rubbing nose and head; 2=puffiness around the eyes and mouth and pilar erecti; 3=decreased activity with increased respiratory rate); (B). Concentration of IgG1 and (C). IgE in plasma; (D). Concentration of IFN- γ in the spleen. Histopathology of the jejunum of the anaphylactic mice (E) BLG + CT in PBS ($n=6$), and the different BALB/c control groups (F) BLG in PBS, (G) CT in PBS, (H) PBS ($n=6$ per group) (scale bar = 100 μm). Arrow (yellow) indicates the detaching epithelial cells.

3.2 | Specific molecular signatures point towards developing gut dysbiosis in cow's milk protein-sensitized BALB/c mice

We undertook unsupervised and supervised multivariate data analysis to compare the polar fecal metabolomes of BALB/c mice receiving BLG and CT in PBS ($n=5$) to those receiving solely PBS ($n=6$) at week 3. No clustering according to sensitization was observed using principal component analysis (PCA-X) (Figure S5), but we could detect molecular discrepancies in supervised orthogonal partial least squares discriminant analysis (OPLS-DA), with excellent Q^2 (0.83), $R^2(Y)$ (0.87), permutation testing and a cross-validated analysis of variance (CV-ANOVA) p -value of $7.6e^{-4}$ (Table S17, Figure S6). From this validated OPLS-DA model, the most contributing molecular components (64/8420) were retained for fragmentation and annotation. Mice receiving BLG and CT displayed higher levels of metabolites associated with the gut microbiome-regulated kynurenine pathway, including picolinic acid, quinolinic acid, xanthurenate and 3-hydroxykynurenine, while also the (xanthurenate+3-hydroxykynurenine)/tryptophan ratio

increased. This, along with higher levels of stercobilin and several metabolites related to the bile acid (BA) metabolism, such as taurine, 3,6-diketocholate, 7-ketodeoxycholate, and $3\alpha,7\alpha$ -dihydroxy-12-oxo-5 β -cholanoic acid, points towards microbial dysbiosis.⁴ Moreover, elevated levels of lactate, 2-hydroxyhexanoate and carnitines (valerylcarnitine and L-carnitine) within the energy metabolism are suggestive of immune activation.³⁷ Finally, the levels of several AAs, guanine, histamine and 1-methylhistamine were elevated. Notably, there were no significant Spearman's correlations between molecular compounds contributing most to the allergic phenotype and immunological parameters (Tables S18–S20).

3.3 | Metabolic alterations suggest persistent dysbiosis and allergic inflammation in cow's milk protein-sensitized BALB/c mice

In week 5, again no discernable clustering was observed between the mice that received BLG and CT in PBS ($n=5$) and those that received PBS alone ($n=6$) (Figure S7). However, we were able

to detect molecular discrepancies using OPLS-DA. Indeed, acceptable Q^2 (0.57), $R^2(Y)$ (0.66), permutation testing, and a cross-validated analysis of variance (CV-ANOVA) p -value of $6.4e^{-2}$ were obtained (Table S17, Figure S8). From the 8420 measured molecular compounds, the most contributing ones ($n=57$) were selected for fragmentation and annotation. In contrast to week 3, where we observed an increase in various BAs, histamine and xanthurenate, these metabolites and creatine exhibited a decrease in week 5, while the levels of guanine increased. This persistent dysbiosis was emphasized by increased levels of the bacterial metabolites sterco-bilin and tryptamine, along with a decreased 7-ketodeoxycholate/cholesterol ratio, and reduced levels of the bacterial tryptophan metabolite 3-indoleacetate. The onset of allergic inflammation was suggested by decreased levels of sphingosine and sphinganine, which have been associated with anti-inflammatory effects mediated by sphingosine-1-phosphate (S1P).³⁸ The presence of inflammation was corroborated by reduced concentrations of the antioxidant metabolites 4-hydroxybenzaldehyde³⁹ and 2-oxindole.⁴⁰ Within the energy metabolism, lowered levels of malate and 2-hydroxyhexanoate implied a continuous immune activation. A borderline significant positive correlation between creatine and IgG1 was noted at week 5 (Table S21).

3.4 | Participant profiles of the pediatric cohort

From May 1st, 2017, to March 31, 2021, a total of 81 children (average age = 2 ± 1.8 years) were included in this study (EC2017/1634). Of these children, 22 were diagnosed with IgE-CMA, 21 were suspected of CMA and therefore on a CMP-free diet, but with a negative diagnostic test (non-IgE-CMA). Ten children with (non-)IgE-CMA were also diagnosed with another IgE-mediated FA (IgE-other), while 15 children suffered only from another IgE-mediated FA. Twenty-three healthy siblings of the recruited patients were included as control group. Among the FA patients, 40 were allergic to a single allergen, while the other 18 were allergic to ≥ 2 allergens. The eliciting allergens were CMP ($n=43$), hen's eggs ($n=20$), nuts ($n=11$), fruit and vegetables ($n=6$), wheat ($n=3$), soy ($n=3$), and fish ($n=3$). Clinical symptoms were related to gastrointestinal ($n=42$), dermal ($n=29$), and respiratory ($n=10$) complaints, with anaphylaxis in severe cases ($n=11$). In total, 23 children exhibited a more severe phenotype, either having multiple FAs ($n=12$), a history of anaphylaxis ($n=3$) or both ($n=8$). Thirty-three patients were diagnosed by open OFCs (Tables S24, S25), for which additional statistical analyses were carried out.

3.5 | Specific molecular signatures are associated with dysbiosis and low-grade inflammation in children with IgE-CMA

To further explore the findings from the acute allergic phases, generated through the longitudinal *in vivo* model, we performed metabolomics on urine and feces obtained from the patient cohort,

resembling the subacute to chronic phase of the disease. We observed no clear clustering of the different patient and control groups using unsupervised PCA-X (Figure S9–S11), whereas supervised OPLS-DA modeling of the fecal polar metabolome data enabled discrimination of children with IgE-CMA, for both the entire cohort and the patients with challenge-confirmed diagnosis, against the healthy control group ($Q^2 > 0.5$; $R^2(Y) > 0.85$; p -value $< .05$ and good permutation testing), but not for the lipidome data ($Q^2 < 0.5$) (Tables S26, 27, Figure S12, S13). Urinary polar metabolome data enabled discrimination, but solely among those with challenge-confirmed diagnosis (Table S28; Figure S14). From the validated OPLS-DA models, the compounds which contributed the most (52 or 100/24,924 fecal (entire cohort or challenge-confirmed) and 74/19,841 urinary molecular compounds (challenge-confirmed) were retained for fragmentation and annotation.

In fecal samples of children with IgE-CMA, similar to the findings in the murine experiment, signs of dysbiosis were clearly noted, more specifically through alterations in the levels of sterco-bilin, BAs and tryptophan and its metabolites. This was reflected also in both the tryptophan (tryptophan metabolites/tryptophan)- and the BA (secondary/primary BAs) ratios, irrespective of the diagnostic method used. Co-occurrence of immune activation in patients with (severe) IgE-CMA was in line with the murine data, also suggested by altered levels of acylcarnitines and fatty acids, belonging to the energy metabolism, next to sphingolipids and glycerophospholipids. Alterations in AAs were also observed and could be linked to either dysbiosis⁴¹ and/or inflammation.⁴² In children with challenge-confirmed IgE-CMA, these shifts were accompanied by elevated concentrations of 2-piperidinone, a compound associated with inflammation (Tables S29–S34). Furthermore, mummichog pathway analysis on data from the entire cohort confirmed altered BA biosynthesis, energy, glycosphingolipid, glycerophospholipid, nucleotide and tryptophan metabolism (Tables S35, S36).

Consistent with the findings in fecal samples from IgE-CMA patients, dysbiosis and inflammation were reflected by predominantly increased urinary AA levels and changes in BAs, energy and tryptophan metabolism. Additionally, the alterations of 2-piperidinone and trimethylamine-N-oxide in (severe) IgE-CMA further supported this, regardless of the diagnostic procedure. Moreover, changes in nucleotide levels, especially in challenge-confirmed cases provided additional corroboration of inflammatory conditions. Mummichog analysis further substantiated these alterations in tryptophan, AA and energy metabolism (Tables S37–S40).

3.6 | IgE-CMA in children is associated with gut microbial dysbiosis

As most of the significantly differing metabolites and lipids originated from abnormal microbial metabolism, we performed additional 16S rRNA gene sequencing on children's fecal samples. We observed a significant difference in α - and β -diversity, regardless of the diagnostic procedure, mainly according to CMP consumption

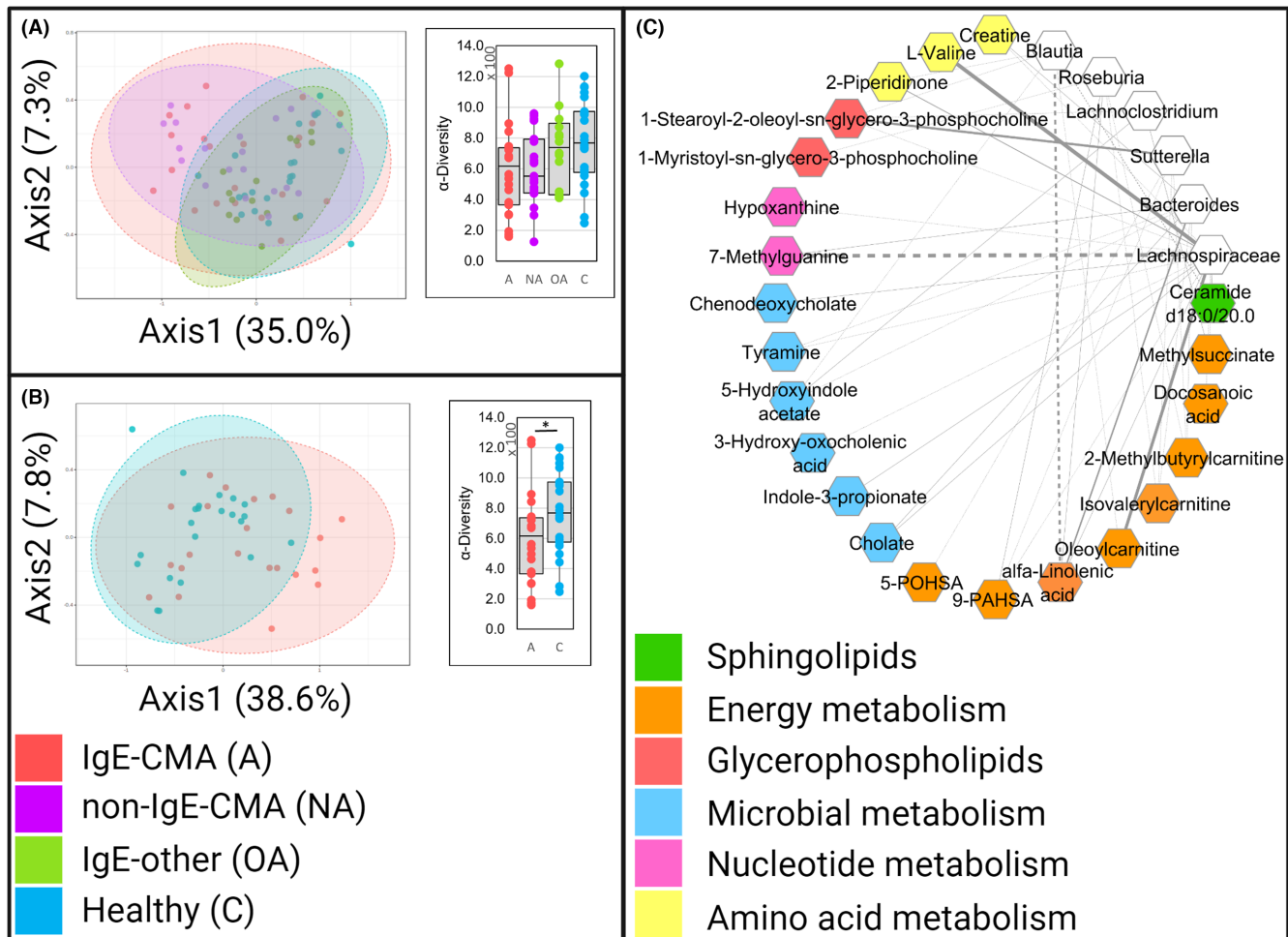


FIGURE 2 (A) PCoA plot with Bray-Curtis distance and total sum normalization and box plot of the α -diversity using Chao1 at OTU level, for the comparison between children with IgE-CMA ($n=22$), children with other IgE-mediated food allergies (IgE other; $n=15$), children with non-IgE-mediated CMA (non-IgE-CMA; $n=21$), and a healthy control group ($n=23$), (B). PCoA plot with Bray-Curtis distance and a box plot of the α -diversity (Chao1) at OTU level, between children with IgE-CMA and the healthy controls, and (C). Spearman correlations (p -value $<.05$ and $\rho >.3$) between our discriminative compounds and microbial OTUs. Dotted line: negative correlations; full line: positive correlation; the thicker the line, the stronger the correlation. * p -value $<.05$.

[(non-)IgE-CMA vs. healthy] (Figure 2A; p -value $<.05$). In this context, no significant differences were observed for α - and β -diversity between children with IgE-CMA and non-IgE-CMA, although pairwise comparisons identified several (borderline) significant operational taxonomic units (OTUs), including *Bacteroides* sp. and *Lachnospiraceae* sp. (Table S41-S44). Conversely, the gut bacterial community composition of children with IgE-CMA significantly differed from healthy controls, both in overall community composition (β -diversity; p -value .006) and in microbial richness (α -diversity (p -value .039)). However, this distinction disappeared when focusing only on challenge-confirmed patients (α and β -diversity; p -value .48 and .29, respectively) (Tables S41,S42). Pairwise comparisons identified borderline significant (p -value $<.10$) OTUs, including enrichment of *Lachnospiraceae* sp. in patients with IgE-CMA, whereas healthy controls harbored more *Faecalibacterium* sp., *Blautia* sp., *Alistipes* sp., *Bacteroides* sp. and *Faecalibacterium* sp. (Figure 2B, Table S45,S46).

3.7 | Gut microbial dysbiosis in children with IgE-CMA is reflected in their gastrointestinal molecular composition

In light of the observed dysbiosis in children with IgE-CMA, we performed an integrative omics analysis to study how significantly varying molecular features (metabolites and lipids) related to altered microbial OTUs using Spearman's correlation, DIABLO, and MOFA. Metabolites associated with IgE-CMA exhibited a positive correlation with *Bacteroides* sp., but an inverse correlation with *Blautia* sp., *Roseburia* sp. and *Sutterella* sp. The correlations with *Lachnospiraceae* sp. were comparatively less consistent (Figure 2C; Tables S47-S49). For metabolites associated with a severe allergic phenotype, an inverse correlation was observed with *Bifidobacterium* sp., *Blautia* sp. and *Sutterella* sp., while correlations with *Lachnospiraceae* sp., *Lachnospira* sp., *Oscillospiraceae* sp. and *Bacteroides* sp. were mainly

positive. Again, correlations with *Lachnospiraceae* sp. were less consistent (Tables S50–S52).

Multi-omics analysis on the entire patient cohort using unsupervised MOFA clearly distinguished the healthy group from the allergic groups (IgE-CMA, non-IgE-CMA, and IgE-other), whereas supervised DIABLO modeling illustrated clustering according to CMP consumption (Figure S15,S16). Focusing solely on challenge-confirmed FA, the division with MOFA was predominantly based on CMP consumption, while DIABLO identified a divergent clustering pattern for IgE-CMA cases (Figure S17,S18). The main drivers of variation included amongst others cholate, sulfolithocholyglycine and sterco-bilin as well as *Lachnospiraceae* sp., *Blautia* sp. and *Lachnoclostridium* sp. (Tables S53–S58).

3.8 | In vitro digestions confirm microbial origin of metabolic changes in children with IgE-CMA

To explore how the gut microbiome impacts the prevalence of detected fecal metabolites, and to further unravel the extent of the observed dysbiosis IgE-CMA allergic children display, we investigated the alterations in the gastrointestinal metabolome following a 48-h gut microbial fermentation. To achieve this, we employed simulated gastrointestinal digestions, including salivary, gastric, and small intestine (including bile) simulations, on commercial CMP formula. Subsequently, we introduced fecal inocula from children with diverse phenotypes (IgE-CMA, IgE-CMA resolution and healthy children), and thus distinct microbial signatures, to observe how the specific microbiota affected the gastrointestinal metabolome. Unsupervised PCA-X modeling showed clustering according to colonic digestion (T0 vs. T48) (Figure S19,S20). In general, BA concentrations decreased following digestion, with the exception of 7-ketodeoxycholate and oxoBAs. Similarly, trimethylamine, trimethylamine-N-oxide, tryptophan and its catabolites increased following digestion, whereas acylcarnitines and other metabolites belonging to the lipid metabolism decreased (Table S59).

4 | DISCUSSION

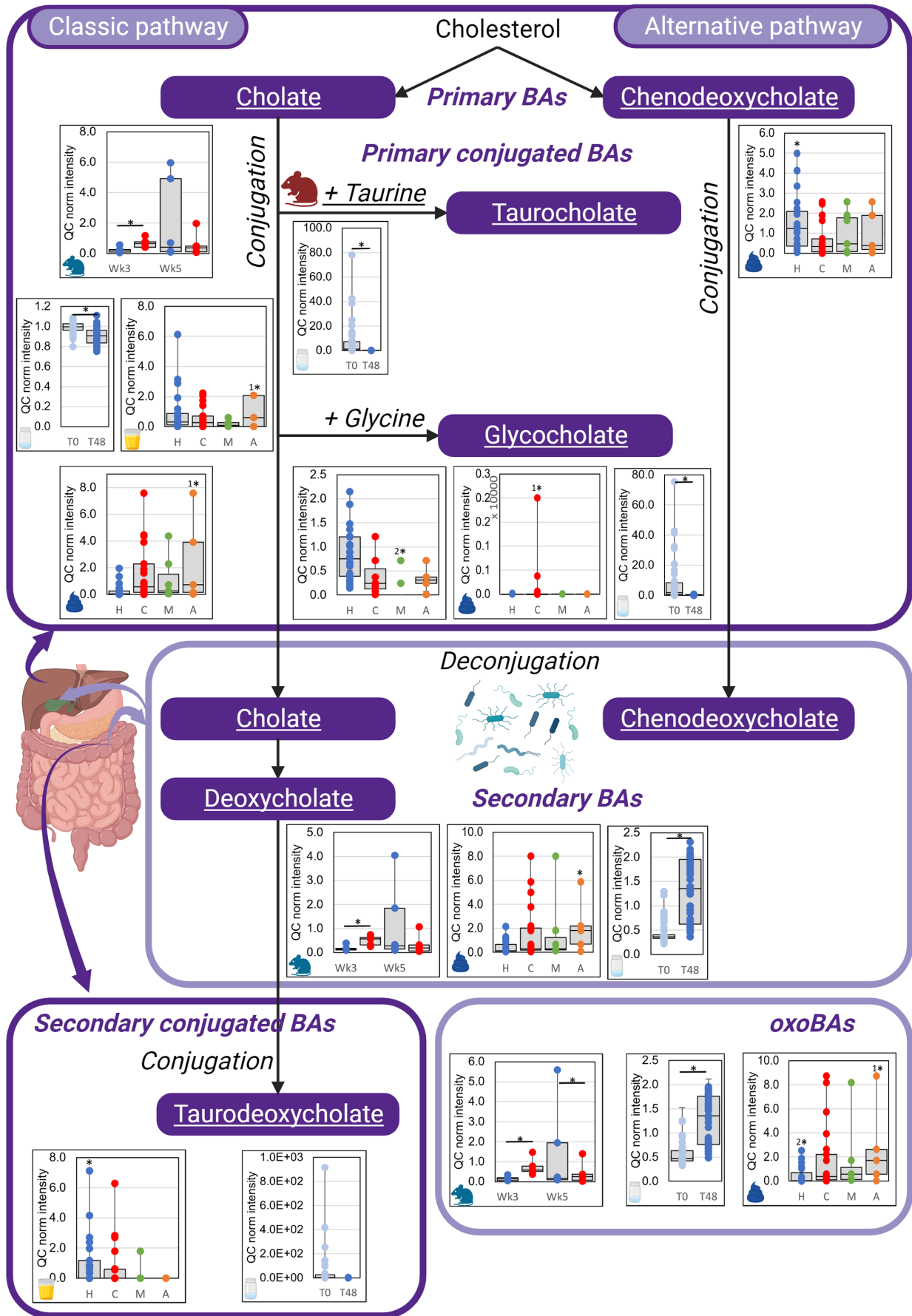
We present a comprehensive study on metabolic pathways underlying IgE-CMA in children. These were revealed by gut metabolomics in a longitudinal murine model, and gut metabolomics, lipidomics, and microbiome analysis in a patient cohort. We identified multiple microbially derived metabolic alterations, suggesting aberrant

microbial composition and functionality. Indeed, gut microbial dysbiosis was observed in our patient cohort and the causality of microbial disturbances was inferred by integrated omics analyses and in vitro colonic digestions. The detected metabolic alterations could be divided into three groups based on their position in our proposed pathophysiological cascade: (1) early-stage microbial metabolites reflective of gut dysbiosis, observed early onwards in the sensitization, that steer the development of the immune system toward FAs; (2) markers of dysbiosis and (allergic) inflammation indicating the onset of IgE-CMA; and (3) markers of dysbiosis, thereby reflecting a sustained chronic inflammation, which were observed in allergic children on an elimination diet.

In the present study, BALB/c mice receiving BLG and CT optimally mimicked the human allergic response as these mice showed signs of anaphylaxis (Figure 1A), and clear alterations in immunological sensitization markers (Figure 1B–D). However, the levels of IFN- γ and IL-4 did not correlate with IgE, which was also observed by De Vooght et al.⁴³ This could be attributed to higher Th2 cytokine production in mesenteric lymph nodes compared to spleen cells, due to the importance of the former in oral tolerance induction.⁴⁴

Already at the first sampling point (week 3), we discovered specific molecular alterations, reflective of microbial dysbiosis in BALB/c mice receiving BLG and CT, using fecal metabolomics. Most importantly, alterations in secondary and oxo-BAs were observed (Figure 3), which are endogenous ligands of the Farnesoid X receptor, the G-protein-coupled receptor (TGR5) and the retinoid-related orphan receptor γ t (ROR γ t), all known for their anti-inflammatory properties through the regulation of T cell responses.^{45,46} BALB/c mice undergoing sensitization also exhibited higher levels of tryptophan metabolites and a higher (xanthurenate+3-hydroxykynurenine)/tryptophan ratio (Figure 4). Tryptophan is an essential aromatic amino acid that is metabolized through three main pathways: (a) the kynurenine pathway, that is, via the rate-limiting indoleamine 2,3-dioxygenase-1 (IDO-1) enzyme; (b) the indolic pathway, that is, direct transformation by the gut microbiota into indolic compounds; and (c) the serotonin pathway, that is, transformation by tryptophan hydroxylase-1 in enterochromaffin cells.^{4,47,48} IDO-1 controls the proliferation and the activity of immune cells, thereby supporting peripheral tolerance.⁴⁹ Both the activity and expression of IDO-1 are induced by bacterial compounds via toll-like receptors. The ratio of tryptophan versus its catabolites is considered as a biomarker of the activated immune system, as elevated tryptophan and lower catabolite levels suggest inactivation of the IDO-1 enzyme.^{4,50} Different kynurenine and indolic metabolites are also known to act as aryl hydrocarbon (AhR)-ligands,⁴⁸ which maintain

FIGURE 3 Cow's milk protein-sensitized BALB/c mice, cow's milk-allergic children, and their in vitro gastrointestinal digests display a differential bile acid (BA) metabolism compared to healthy controls. Concentrations of primary BAs, primary conjugated BAs, secondary BAs, secondary conjugated BAs and oxoBAs (3 α ,7 α -dihydroxy-12-oxo-5 β -cholanoic acid) in the gut in our IgE-CMA cohort (healthy (blue; H), IgE-CMA (red; C), multiple FAs (green; M) and a history of anaphylaxis (orange; A), murine models (IgE-CMA (red), healthy (blue)), and in vitro digests before (light blue; T0) and after (dark blue; T48) colonic digestion. Underlined metabolites represent metabolic alterations (concentrations of taurine are not visualized, but increased in sensitized mice [red mouse]). * in all data: p -value $<$.10; in patient cohort, conditions 1 and 2: 1* in condition 1 (all diagnosis combined) p -value $<$.10; 2* in condition 2 (challenge-confirmed IgE-CMA) p -value $<$.10.



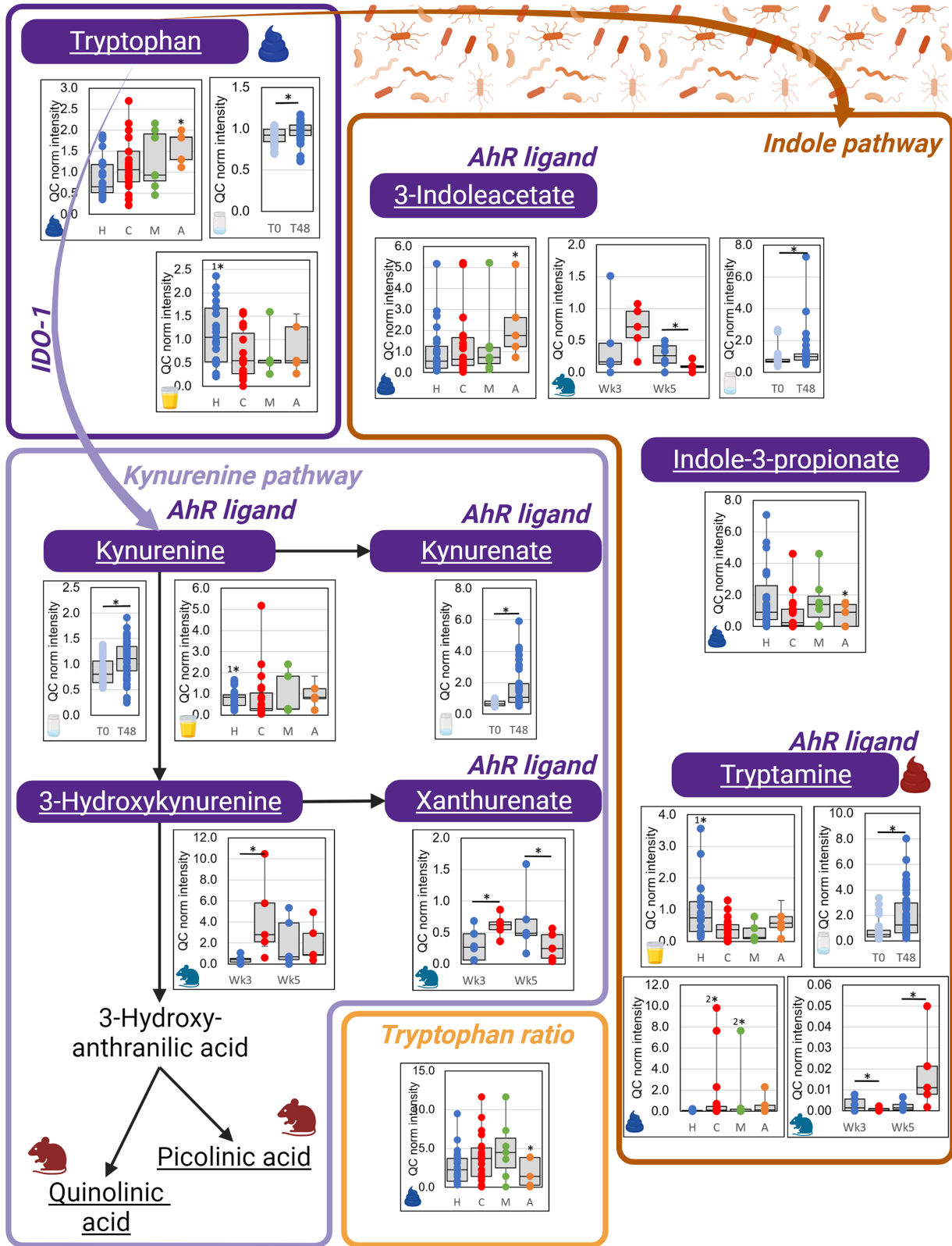


FIGURE 4 Cow's milk protein-sensitized BALB/c mice, cow's milk-allergic children, and their in vitro gastrointestinal digests present a differential tryptophan metabolism. Overview of the kynurenine pathway, indole pathway and serotonin pathway in our IgE-CMA cohort (healthy (blue; H), IgE-CMA (red; C), multiple FAs (green; M) and a history of anaphylaxis (orange; A), murine models (IgE-CMA (red) (blue)), and in vitro digests before (light blue; T0) and after (dark blue; T48) colonic digestion. Underlined metabolites represent metabolic alterations (concentrations of picolinic acid and quinolinic acid are not visualized, but increased in sensitized mice [red mouse]). (Tryptophan ratio: (xanthurenate + 3-hydroxykynurenine + kynurenine + kynurenate)/tryptophan) * in all data: p -value $< .10$; in patient cohort, conditions 1 and 2: 1* in condition 1 (all diagnosis combined) p -value $< .10$; 2* in condition 2 (challenge-confirmed IgE-CMA) p -value $< .10$.

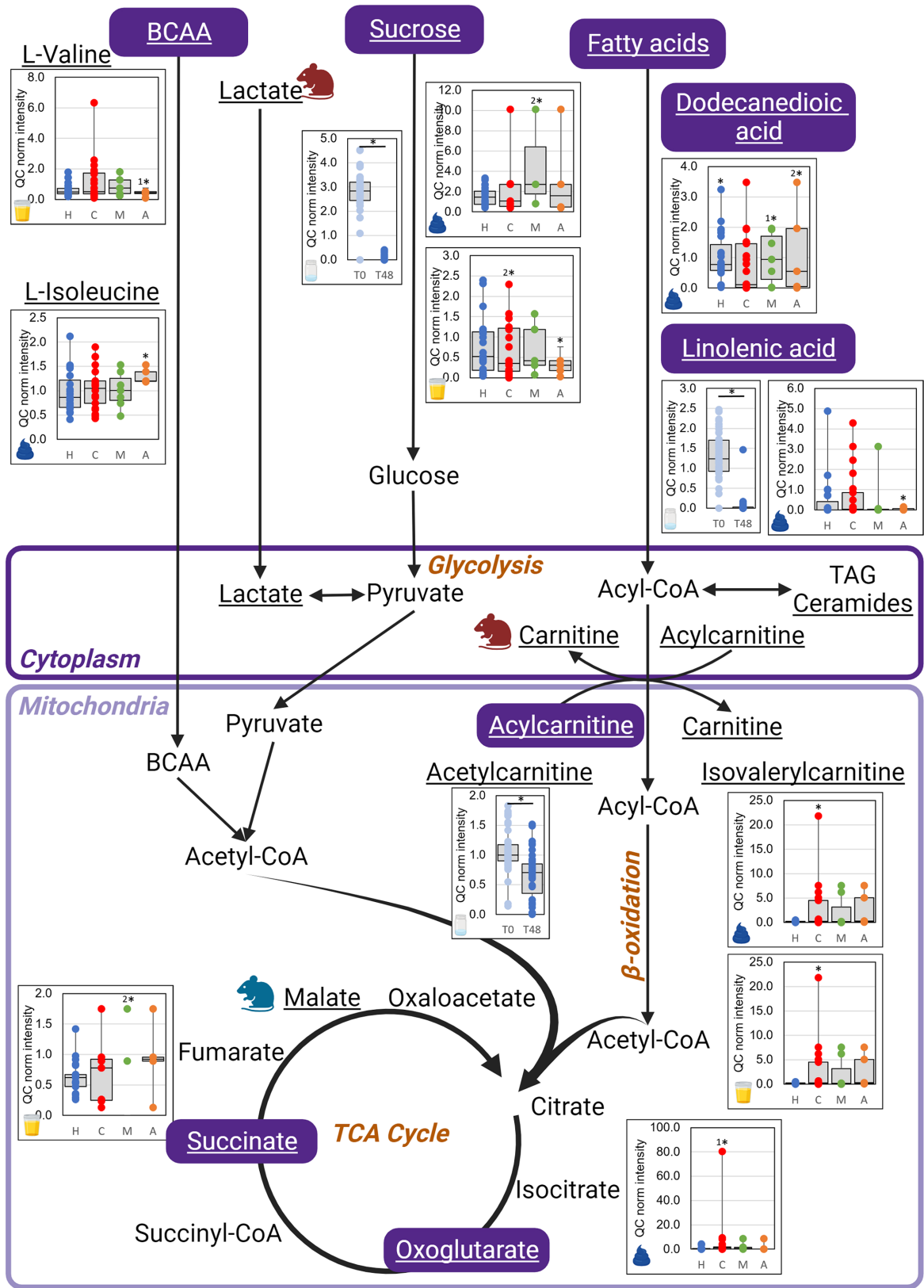


FIGURE 5 Cow's milk protein-sensitized BALB/c mice, cow's milk-allergic children, and their in vitro gastrointestinal digests present a differential energy metabolism. Overview of the energy metabolism in our IgE-CMA cohort (healthy (blue; H), IgE-CMA (red; C), multiple FAs (green; M) and a history of anaphylaxis (orange; A)), murine models (IgE-CMA (red), healthy (blue)), and in vitro digests before (light blue; T0) and after (dark blue; T48) colonic digestion. Underlined metabolites represent metabolic alterations (concentrations of carnitine, malate and lactate, are not visualized, but increased (red mouse) or decreased (blue mouse) in sensitized mice). * in all data: p -value $< .10$; in patient cohort, conditions 1 and 2: 1* in condition 1 (all diagnosis combined) p -value $< .10$; 2* in condition 2 (challenge-confirmed IgE-CMA) p -value $< .10$.

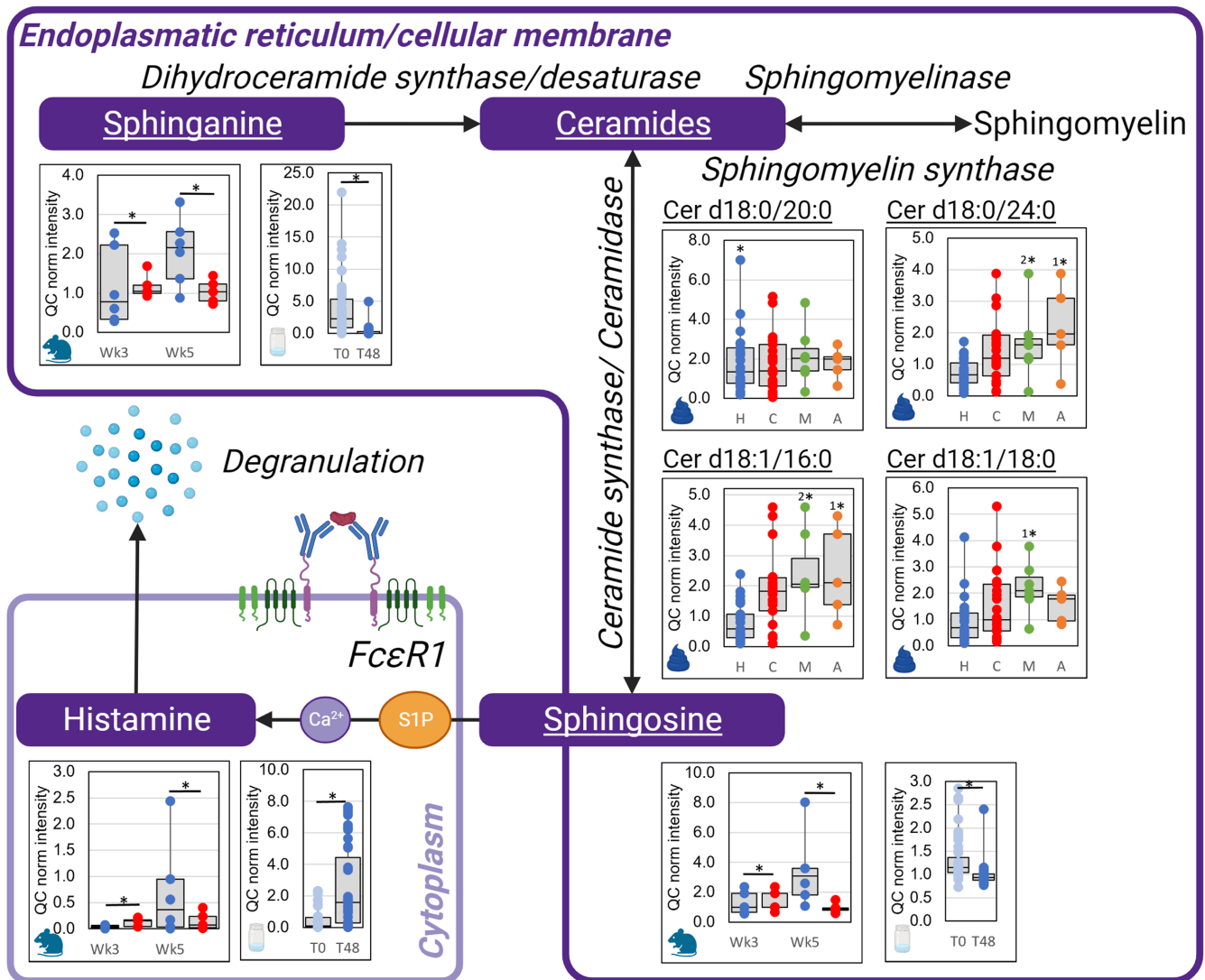


FIGURE 6 Cow's milk protein-sensitized BALB/c mice, cow's milk-allergic children, and their in vitro gastrointestinal digests present a differential sphingolipid metabolism. Overview of the sphingolipid metabolism between IgE-CMA and control groups in our IgE-CMA cohort (feces, urine; healthy control group (blue; H), children with IgE-CMA (red; C), children with multiple FAs (green; M) and children with a history of anaphylaxis (orange; A), murine models (mouse; IgE-CMA (red), healthy (blue)), and in vitro digests before (light blue; T0) and after (dark blue; T48) colonic digestion. S1P: Sphingosine-1-phosphate; * in all data: p -value $< .10$; in patient cohort, conditions 1 and 2: 1* in condition 1 (all diagnosis combined) p -value $< .10$; 2* in condition 2 (challenge-confirmed IgE-CMA) p -value $< .10$.

intestinal homeostasis through mediation of both innate and adaptive immune responses.^{4,51} In this regard, shifts within the tryptophan metabolism reflect intestinal permeability and host immunity effects as well.⁴⁸ Alterations in the energy metabolism were also observed (Figure 5), which presumably reflect immune activation, as rapidly dividing and proliferating activated immune cells turn to aerobic glycolysis to ensure adequate energy supply.³⁷ Next to an increased energy need for the immune system, a dysregulated energy supply could result from gut dysbiosis. Under normal conditions, the production of butyrate and other short-chain fatty acids as energy source leads to increased colonic Forkhead box P3 (Foxp3+) Treg cells, thereby suppressing colonic inflammation and effectuating a shift from glycolysis to fatty acid metabolism.⁵²

In the second phase of the sensitization, that is, week 5, a continued dysbiosis, steering the immune system towards FA was evident through alterations in BAs, but also the tryptophan and energy metabolism. Indeed, a dysbiosis-driven allergic inflammation was endorsed by substantial effects at the level of the sphingolipid metabolism, with significantly lower levels of sphinganine and sphingosine in sensitized BALB/c mice (Figure 6). In general, sphingolipids are synthesized de novo, but they can also be derived from dietary sources and produced by *Bacteroides* species in the gut.¹⁶ Sphingolipids have an important function in inflammation and immunity as mast cell regulators, through the formation of S1P.¹⁶ The decline in sphinganine and sphingosine in CMP-allergic mice causes a dysregulation of the innate immune

system and mast cell metabolism, accompanied by the onset of allergic inflammation.¹⁶ Indeed, S1P has been reported to have an immune-regulatory role, and is associated with many inflammatory conditions, such as asthma and autoimmunity.⁵³ The presence of inflammatory conditions was further corroborated by decreased levels of the antioxidant metabolites 4-hydroxybenzaldehyde³⁹ and 2-oxindole.⁴⁰

Ultimately, our goal was to ascertain whether the acute changes associated with sensitization (week 3) and allergic inflammation (week 5) in sensitized mice could be detected at a subacute to chronic disease stage in children as well, particularly in those adhering to an elimination diet. Indeed, we successfully confirmed the aforementioned microbial dysbiosis through altered fecal levels of BAs of the classic pathway and a dysregulated metabolization from primary to secondary BAs (Figure 3). Next to their immunoregulatory role, BAs are key in maintaining the symbiotic communication between the host and its microbiome.⁴⁵ This interplay was confirmed by *in vitro* gastrointestinal digestions, displaying formation of the secondary BA 7-ketodeoxycholate and oxoBAs, and integrative omics analysis, highlighting correlations between BAs and *Lachnospiraceae* sp., *Faecalibacterium* sp. and others (Figure 3). We further confirmed gut dysbiosis through the observation of altered fecal (and urinary) tryptophan and catabolite levels (Figure 4) and urinary trimethylamine-N-oxide. Furthermore, we substantiated the presence of inflammation by detecting elevated levels of 2-piperidinone in both urine and feces of allergic children. Even more, the ongoing dysbiosis perpetuates a chronic low-grade inflammation, as evidenced by alterations in the energy and urinary nucleotide metabolism (Figure 5). Indeed, both the gastrointestinal digestions and multi-omics analysis highlighted correlations between acylcarnitines and urinary nucleotides on the one hand, and short-chain fatty acid-producing gut bacteria belonging to *Bacteroides* sp. and the *Lachnospiraceae* family on the other hand. Although increased levels of the nucleotide guanine were already observed during sensitization in mice, the impact of IgE-CMA on the nucleotide metabolism was even more prominent in our patient cohort. In allergic children, not only were higher levels of urinary guanine linked to IgE-CMA severity, but enrichment of xanthine, xanthosine, uridine, adenosine, inosine and methylguanine was also observed, although only in patients with challenge-confirmed IgE-CMA. Purines and pyrimidines participate in the purinergic signaling complex, impacting immunity and inflammation, by eliciting diverse responses in inflammatory cells.⁵⁴ This inflammation was further corroborated by changes in fecal sphingolipids and glycerophospholipids. Higher fecal ceramide levels were also present in severely allergic children (Figure 6), which might reflect an impaired synthesis of sphingomyelins and S1P. This conversion could be associated with increased mast cell responsiveness towards a hyperresponsive state.¹⁶ Alterations in glycerophospholipids, associated with IgE-CMA (severity) were also observed by Kong et al.⁵⁵ and Chalcraft et al.,⁵⁶ who reported changes in serum glycerophospholipids before and in the early and late phase of anaphylaxis in mice. As these compounds are the main constituents of cellular

membranes and chemically similar to the platelet-activating-factor, they could play a role in the initiation of allergic reactions.⁴

In this study, the main goal was to elucidate metabolic alterations underlying IgE-CMA in children. For this purpose, initial hypotheses regarding the acute allergic phase were generated using a longitudinal murine *in vivo* model, while the subacute to chronic stage was further investigated in a pediatric patient cohort. For those metabolic alterations that could be correlated to the gut microbiome, causality was inferred using *in vitro* gastrointestinal digestions and a multi-omics approach. This empowered an in-depth understanding of metabolic changes underlying the pathophysiology of IgE-CMA, despite not including allergic children who were still consuming the triggering antigen, or a sensitized-only control group. The decision to omit these groups was primarily based on practical considerations, as most parents eliminate the specific antigens from the diet when their children are suspected of having this condition. Nevertheless, we collected samples as promptly as possible following diagnosis. Consequently, our interpretation of the patient data was confined to the disease's steady state, as it reflected the condition after the elimination diet had been implemented. In the case of the murine experiment, we adhered to the 3R principle, which emphasizes the principles of Replacement, Reduction, and Refinement in animal research. As a result, mice were euthanized, and samples were collected solely at the end of the experiment. This limitation implies that we do not have measurements of antibodies, cytokines or histology available during the sensitization phase.

Together, however, the metabolic and microbial signatures and their causal linkages we report here for pediatric IgE-CMA constitute a comprehensive resource that can guide follow-up studies aimed at designing prevention and treatment strategies.

AUTHOR CONTRIBUTIONS

Conceptualization: E.D.P., D.B., L.V., E.C., L.V.; patient recruitment: E.D.P., N.B., D.B., T.C., K.K., A.N., K.V., M.V.W., L.V.; methodology: E.D.P., D.B., T.V.D.W., W.V.D.B., L.V., E.C., L.V.; experimental work: E.D.P., V.P.; statistical analysis: E.D.P., V.P., M.D.G., P.V.; writing: E.D.P., C.E., L.V.

ACKNOWLEDGMENTS

Ellen De Paepe (FWO, 1S49020N) and Dominique Bullens (FWO, 1801019N) are supported by Research Foundation – Flanders. Vera Plekhova (24Y2019003001) is supported by the Special Research Fund of Ghent University. The Laboratory of Integrative Metabolomics research group is part of the Ghent University expertise center MSsmall. The manuscript was written with the contributions of all authors. All authors have given approval for the final version of the manuscript. The authors wish to thank D. Stockx, B. Pomian, J. Goedgebuer, M. Naessens, T. De Troyer, JP. Ottoy, S. Kamelouroumieh, G. Blancke, T. Lacoere, L. De Bels, S. Brabant, H. Viljakainen, and S. Raju for their contribution to this work.

CONFLICT OF INTEREST STATEMENT

The authors declare no competing interests.

DATA AVAILABILITY STATEMENT

The raw UHPLC-HRMS data generated in this study have been deposited in the Metabolomics Workbench database under accession numbers ST002985 (in vitro data), ST002944 (polar metabolomics feces mice), ST002945 (polar metabolomics feces patients), ST002946 (lipidomics feces patients) and ST002988 (polar metabolomics urine patients). All other data are available from the corresponding author on reasonable request.

ORCID

Lynn Vanhaecke  <https://orcid.org/0000-0003-0400-2188>

REFERENCES

- Flom JD, Sicherer SH. Epidemiology of Cow's Milk allergy. *Nutrients*. 2019;11:1051. doi:10.3390/NU11051051
- Bilaver LA, Chadha AS, Doshi P, O'Dwyer L, Gupta RS. Economic burden of food allergy: a systematic review. *Ann Allergy Asthma Immunol*. 2019;122(4):373-380.e1. doi:10.1016/J.ANAI.2019.01.014
- Carucci L, Nocerino R, Paparo L, Di Scala C, Berni CR. Dietary prevention of atopic march in pediatric subjects with Cow's Milk allergy. *Front Pediatr*. 2020;8:440. doi:10.3389/FPED.2020.00440/BIBTEX
- De Paepe E, Van GL, De Spiegeleer M, et al. A systematic review of metabolic alterations underlying IgE-mediated food allergy in children. *Mol Nutr Food Res*. 2021;65(23):2100536. doi:10.1002/MNFR.202100536
- De Filippis F, Paparo L, Nocerino R, et al. Specific gut microbiome signatures and the associated pro-inflammatory functions are linked to pediatric allergy and acquisition of immune tolerance. *Nat Comm*. 2021;12(1):1-11. doi:10.1038/s41467-021-26266-z
- Thompson-Chagoyan OC, Fallani M, Maldonado J, et al. Faecal microbiota and short-chain fatty acid levels in faeces from infants with cow's milk protein allergy. *Int Arch Allergy Immunol*. 2011;156(3):325-332. doi:10.1159/000323893
- Thompson-Chagoyan OC, Vieites JM, Maldonado J, Edwards C, Gil A. Changes in faecal microbiota of infants with cow's milk protein allergy - a Spanish prospective case-control 6-month follow-up study. *Pediatr Allergy Immunol*. 2010;21(2 PART 2):e394-e400. doi:10.1111/J.1399-3038.2009.00961.X
- Bunyavanich S, Shen N, Grishin A, et al. Early-life gut microbiome composition and milk allergy resolution. *J Allergy Clin Immunol*. 2016;138(4):1122-1130. doi:10.1016/J.JACI.2016.03.041
- Feehley T, Plunkett CH, Bao R, et al. Healthy infants harbor intestinal bacteria that protect against food allergy. *Nat Med*. 2019;25(3):448-453. doi:10.1038/s41591-018-0324-z
- Rodriguez B, Prioult G, Hacini-Rachinel F, et al. Infant gut microbiota is protective against cow's milk allergy in mice despite immature ileal T-cell response. *FEMS Microbiol Ecol*. 2012;79(1):192-202. doi:10.1111/J.1574-6941.2011.01207.X
- Noval Rivas M, Burton OT, Wise P, et al. A microbiota signature associated with experimental food allergy promotes allergic sensitization and anaphylaxis. *J Allergy Clin Immunol*. 2013;131(1):201-212. doi:10.1016/J.JACI.2012.10.026
- Canani RB, Sangwan N, Stefka AT, et al. Lactobacillus rhamnosus GG-supplemented formula expands butyrate-producing bacterial strains in food allergic infants. *The ISME Journal*. 2015;10(3):742-750. doi:10.1038/ismej.2015.151
- Abdel-Gadir A, Stephen-Victor E, Gerber GK, et al. Microbiota therapy acts via a regulatory T cell MyD88/ROR γ t pathway to suppress food allergy. *Nat Med*. 2019;25(7):1164-1174. doi:10.1038/s41591-019-0461-z
- Lee-Sarwar K, Kelly RS, Lasky-Su J, et al. Intestinal microbial-derived sphingolipids are inversely associated with childhood food allergy. *J Allergy Clin Immunol*. 2018;142(1):335-338.e9. doi:10.1016/j.jaci.2018.04.016
- Savage JH, Lee-Sarwar KA, Sordillo J, et al. A prospective microbiome-wide association study of food sensitization and food allergy in early childhood. *Allergy*. 2018;73(1):145-152. doi:10.1111/ALL.13232
- Crestani E, Harb H, Charbonnier LM, et al. Untargeted metabolomic profiling identifies disease-specific signatures in food allergy and asthma. *J Allergy Clin Immunol*. 2020;145(3):897-906. doi:10.1016/j.jaci.2019.10.014
- Beger RD, Dunn W, Schmidt MA, et al. Metabolomics enables precision medicine: "a white paper, community perspective". *Metabolomics*. 2016;12(10):149. doi:10.1007/s11306-016-1094-6
- Bao R, Hesser LA, He Z, Zhou X, Nadeau KC, Nagler CR. Faecal microbiome and metabolome differ in healthy and food-allergic twins. *J Clin Invest*. 2021;131(2):e141935. doi:10.1172/JCI141935
- Zierer J, Jackson MA, Kastenmüller G, et al. The fecal metabolome as a functional readout of the gut microbiome. *Nature Genetics*. 2018;50(6):790-795. doi:10.1038/s41588-018-0135-7
- Adel-Patient K, Bernard H, Ah-Leung S, Créminon C, Wal JM. Peanut- and cow's milk-specific IgE, Th2 cells and local anaphylactic reaction are induced in Balb/c mice orally sensitized with cholera toxin. *Allergy*. 2005;60(5):658-664. doi:10.1111/J.1398-9995.2005.00767.X
- Shindo T, Kanazawa Y, Saito Y, Kojima K, Ohsawa M, Teshima R. Effective induction of oral anaphylaxis to ovalbumin in mice sensitized by feeding of the antigen with aid of oil emulsion and salicylate. *J Toxicol Sci*. 2012;37(2):307-315. doi:10.2131/JTS.37.307
- Santos AF, Riggioni C, Agache I, et al. EAACI guidelines on the diagnosis of IgE-mediated food allergy. *Allergy*. 2023;10:3057-3076. doi:10.1111/ALL.15902
- Van Hecke T, Vanden Bussche J, Vanhaecke L, Vossen E, Van Camp J, De Smet S. Nitrite curing of chicken, pork, and beef inhibits oxidation but does not affect N-nitroso compound (NOC)-specific DNA adduct formation during in vitro digestion. *J Agric Food Chem*. 2014;62(8):1980-1988. doi:10.1021/jf4057583
- Rombouts C, Hemeryck LY, Van Hecke T, De Smet S, De Vos WH, Vanhaecke L. Untargeted metabolomics of colonic digests reveals kynurenine pathway metabolites, dityrosine and 3-dehydrocarnitine as red versus white meat discriminating metabolites. *Sci Rep*. 2017;7:1-13. doi:10.1038/srep42514
- De Paepe E, Van Meulebroek L, Rombouts C, et al. A validated multi-matrix platform for metabolomic fingerprinting of human urine, feces and plasma using ultra-high performance liquid-chromatography coupled to hybrid orbitrap high-resolution mass spectrometry. *Anal Chim Acta*. 2018;1033:108-118. doi:10.1016/j.aca.2018.06.065
- Van Meulebroek L, De Paepe E, Verduyck V, et al. Holistic Lipidomics of the human gut phenotype using validated ultra-high-performance liquid chromatography coupled to hybrid Orbitrap mass spectrometry. *Anal Chem*. 2017;89(22):12502-12510. doi:10.1021/acs.analchem.7b03606
- Vanden Bussche J, Marzorati M, Laukens D, Vanhaecke L. Validated high resolution mass spectrometry-based approach for Metabolomic fingerprinting of the human gut phenotype. *Anal Chem*. 2015;87(21):10927-10934. doi:10.1021/acs.analchem.5b02688
- Wang Q, Garrity GM, Tiedje JM, Cole JR. Naïve Bayesian classifier for rapid assignment of rRNA sequences into the new

- bacterial taxonomy. *Appl Environ Microbiol*. 2007;73(16):5261-5267. doi:[10.1128/AEM.00062-07](https://doi.org/10.1128/AEM.00062-07)
29. de Jonge NF, Louwen JJR, Chekmeneva E, et al. MS2Query: reliable and scalable MS2 mass spectra-based analogue search. *Nature Communications*. 2023;14(1):1-12. doi:[10.1038/s41467-023-37446-4](https://doi.org/10.1038/s41467-023-37446-4)
 30. Dührkop K, Fleischauer M, Ludwig M, et al. SIRIUS 4: a rapid tool for turning tandem mass spectra into metabolite structure information. *Nat Methods*. 2019;16(4):299-302. doi:[10.1038/S41592-019-0344-8](https://doi.org/10.1038/S41592-019-0344-8)
 31. Pang Z, Chong J, Zhou G, et al. MetaboAnalyst 5.0: narrowing the gap between raw spectra and functional insights. *Nucleic Acids Res*. 2021;49(W1):W388-W396. doi:[10.1093/NAR/GKAB382](https://doi.org/10.1093/NAR/GKAB382)
 32. Chong J, Liu P, Zhou G, Xia J. Using MicrobiomeAnalyst for comprehensive statistical, functional, and meta-analysis of microbiome data. *Nature Protocols*. 2020;15(3):799-821. doi:[10.1038/s41596-019-0264-1](https://doi.org/10.1038/s41596-019-0264-1)
 33. Asnicar F, Berry SE, Valdes AM, et al. Microbiome connections with host metabolism and habitual diet from 1,098 deeply phenotyped individuals. *Nat Med*. 2021;27(2):321-332. doi:[10.1038/S41591-020-01183-8](https://doi.org/10.1038/S41591-020-01183-8)
 34. Argelaguet R, Velten B, Arnol D, et al. Multi-omics factor analysis—a framework for unsupervised integration of multi-omics data sets. *Mol Syst Biol*. 2018;14(6):e8124. doi:[10.15252/MSB.20178124](https://doi.org/10.15252/MSB.20178124)
 35. Singh A, Shannon CP, Gautier B, et al. DIABLO: an integrative approach for identifying key molecular drivers from multi-omics assays. *Bioinformatics*. 2019;35(17):3055-3062. doi:[10.1093/BIOINFORMATICS/BTY1054](https://doi.org/10.1093/BIOINFORMATICS/BTY1054)
 36. Wilson LM, Baldwin AL. Environmental stress causes mast cell degranulation, endothelial and epithelial changes, and edema in the rat intestinal mucosa. *Microcirculation*. 1999;6(3):189-198. doi:[10.1111/J.1549-8719.1999.TB00101.X](https://doi.org/10.1111/J.1549-8719.1999.TB00101.X)
 37. Obeso D, Mera-Berriatua L, Rodríguez-Coira J, et al. Multi-omics analysis points to altered platelet functions in severe food-associated respiratory allergy. *Allergy: European J Allergy Clin Immunol*. 2018;73(11):2137-2149. doi:[10.1111/all.13563](https://doi.org/10.1111/all.13563)
 38. Fettel J, Kühn B, Guillen NA, et al. Sphingosine-1-phosphate (S1P) induces potent anti-inflammatory effects in vitro and in vivo by S1P receptor 4-mediated suppression of 5-lipoxygenase activity. *FASEB J*. 2019;33(2):1711-1726. doi:[10.1096/FJ.201800221R](https://doi.org/10.1096/FJ.201800221R)
 39. Kang CW, Han YE, Kim J, Oh JH, Cho YH, Lee EJ. 4-Hydroxybenzaldehyde accelerates acute wound healing through activation of focal adhesion signalling in keratinocytes. *Sci Rep*. 2017;7(1):14192. doi:[10.1038/s41598-017-14368-y](https://doi.org/10.1038/s41598-017-14368-y)
 40. Rindhe SS, Karale BK, Gupta RC, Rode MA. Synthesis, Antimicrobial and Antioxidant Activity of Some Oxindoles. *Indian J Pharm Sci*. 2011;73(3):292-298.
 41. Belizário JE, Faintuch J, Garay-Malpartida M. Review Article Gut Microbiome Dysbiosis and Immunometabolism: New Frontiers for Treatment of Metabolic Diseases. 2018. doi:[10.1155/2018/2037838](https://doi.org/10.1155/2018/2037838), 2018.
 42. He F, Wu C, Li P, Li N, Zhang D, Zhu Q, Ren W, Peng Y Functions and Signaling Pathways of Amino Acids in Intestinal Inflammation, 2018. doi:[10.1155/2018/9171905](https://doi.org/10.1155/2018/9171905), 2018, 1–13.
 43. de Vooght V, Vanoirbeek JAJ, Luyts K, Haenen S, Nemery B, Hoet PHM. Choice of mouse strain influences the outcome in a mouse model of chemical-induced asthma. *PLoS One*. 2010;5(9):e12581. doi:[10.1371/JOURNAL.PONE.0012581](https://doi.org/10.1371/JOURNAL.PONE.0012581)
 44. Qu C, Srivastava K, Ko J, Zhang TF, Sampson HA, Li XM. Induction of tolerance after establishment of peanut allergy by the food allergy herbal formula-2 is associated with up-regulation of interferon- γ . *Clin Exp All*. 2007;37(6):846-855. doi:[10.1111/J.1365-2222.2007.02718.X](https://doi.org/10.1111/J.1365-2222.2007.02718.X)
 45. Perino A, Demagry H, Velazquez-Villegas L, Schoonjans K. Molecular physiology of bile acid signaling in health, disease, and aging. *Physiol Rev*. 2021;101(2):683-731. doi:[10.1152/PHYSREV.00049.2019](https://doi.org/10.1152/PHYSREV.00049.2019)
 46. Biagioli M, Marchianò S, Carino A, et al. Bile acids activated receptors in inflammatory bowel disease. *Cell*. 2021;10(6):1281. doi:[10.3390/CELLS10061281](https://doi.org/10.3390/CELLS10061281)
 47. Zelante T, Iannitti RG, Cunha C, et al. Tryptophan catabolites from microbiota engage aryl hydrocarbon receptor and balance mucosal reactivity via interleukin-22. *Immunity*. 2013;39(2):372-385. doi:[10.1016/J.IMMUNI.2013.08.003](https://doi.org/10.1016/J.IMMUNI.2013.08.003)
 48. Agus A, Planchais J, Sokol H. Gut microbiota regulation of tryptophan metabolism in health and disease. *Cell Host Microbe*. 2018;23(6):716-724. doi:[10.1016/j.chom.2018.05.003](https://doi.org/10.1016/j.chom.2018.05.003)
 49. Raitala A, Karjalainen J, Oja SS, Kosunen TU, Hurme M. Indoleamine 2,3-dioxygenase (IDO) activity is lower in atopic than in non-atopic individuals and is enhanced by environmental factors protecting from atopy. *Mol Immunol*. 2006;43(7):1054-1056. doi:[10.1016/j.molimm.2005.06.022](https://doi.org/10.1016/j.molimm.2005.06.022)
 50. Buyuktiryaki B, Sahiner UM, Girgin G, et al. Low indoleamine 2,3-dioxygenase activity in persistent food allergy in children. *Allergy. European J Allergy Clin Immunol*. 2016;71(2):258-266. doi:[10.1111/all.12785](https://doi.org/10.1111/all.12785)
 51. Van der Leek AP, Yanishevsky Y, Kozyrskiy AL. The kynurenine pathway as a novel link between allergy and the gut microbiome. *Front Immunol*. 2017;8:1374. doi:[10.3389/FIMMU.2017.01374/BIBTEX](https://doi.org/10.3389/FIMMU.2017.01374/BIBTEX)
 52. Chinthrajah RS, Hernandez JD, Boyd SD, Galli SJ, Nadeau KC. Molecular and cellular mechanisms of food allergy and food tolerance. *J Allergy Clin Immunol*. 2016;137(4):984-997. doi:[10.1016/J.JACI.2016.02.004](https://doi.org/10.1016/J.JACI.2016.02.004)
 53. Rivera J, Proia RL, Olivera A. The alliance of sphingosine-1-phosphate and its receptors in immunity. *Nat Rev Immunol*. 2008;8(10):753-763. doi:[10.1038/nri2400](https://doi.org/10.1038/nri2400)
 54. Antonioli L, Blandizzi C, Pacher P, Haskó G. The purinergic system as a pharmacological target for the treatment of immune-mediated inflammatory diseases. *Pharmacol Rev*. 2019;71(3):345-382. doi:[10.1124/PR.117.014878](https://doi.org/10.1124/PR.117.014878)
 55. Kong J, Chalcraft K, Mandur TS, et al. Comprehensive metabolomics identifies the alarmin uric acid as a critical signal for the induction of peanut allergy. *European J Allergy Clin Immunol*. 2015;70(5):495-505. doi:[10.1111/all.12579](https://doi.org/10.1111/all.12579)
 56. Chalcraft KR, Kong J, Wasserman S, Jordana M, McCarty BE. Comprehensive metabolomic analysis of peanut-induced anaphylaxis in a murine model. *Metabolomics*. 2014;10(3):452-460. doi:[10.1007/s11306-013-0589-7](https://doi.org/10.1007/s11306-013-0589-7)

SUPPORTING INFORMATION

Additional supporting information can be found online in the Supporting Information section at the end of this article.

How to cite this article: De Paepe E, Plekhova V, Vangeenderhuysen P, et al. Integrated gut metabolome and microbiome fingerprinting reveals that dysbiosis precedes allergic inflammation in IgE-mediated pediatric cow's milk allergy. *Allergy*. 2024;00:1-15. doi:[10.1111/all.16005](https://doi.org/10.1111/all.16005)